Plasma generation by inductive coupling with a planar resonant RF network antenna

2012 J. Phys. D: Appl. Phys. 45 082001

(http://iopscience.iop.org/0022-3727/45/8/082001)

IOP PUBLISHING
IOP FTC
JOURNAL OF PHYSICS D: APPLIED PHYSICS
J. Phys. D: Appl. Phys. **45** (2012) 082001 (5pp)
doi:10.1088/0022-3727/45/8/082001

FAST TRACK COMMUNICATION

Plasma generation by inductive coupling with a planar resonant RF network antenna

S Lecoultre[1], Ph Guittienne[2], A A Howling[1], P Fayet[3] and Ch Hollenstein[1]

[1] Ecole Polytechnique Fédérale de Lausanne (EPFL), Centre de Recherches en Physique des Plasmas, CH-1015 Lausanne, Switzerland
[2] Helyssen, Route de la Louche 31, CH-1092 Belmont-sur-Lausanne, Switzerland
[3] Tetra Pak (Suisse) SA, D&E, Advanced Film and Barrier Solutions, CP 32, CH-1680 Romont, Switzerland

E-mail: guittienne@helyssen.com

Received 7 December 2011, in final form 31 January 2012
Published 10 February 2012
Online at stacks.iop.org/JPhysD/45/082001

Abstract
A planar antenna operating at 13.56 MHz is presented for potential applications in plasma processing. It consists of interconnected elementary resonant meshes composed of inductive and capacitive elements. Due to its structure, the antenna exhibits a set of resonant modes associated with peaks of the real input impedance. Each mode is defined by its particular distribution of current and voltage oscillating at the frequency of the mode. A rectangular antenna of 0.55 m × 0.20 m has been built and first results obtained with argon plasmas are presented. Efficient plasma generation is shown by plasma densities above 3×10^{17} m^{-3} at 2000 W with reasonable uniformity over the antenna area. The plasma couples inductively with the resonating currents flowing in the antenna above a threshold power of about 60 W. The real input impedance at antenna resonance avoids the problem of strong reactive currents and voltages in the matching box and RF power connections associated with conventional large-area plasma sources. Resonant RF networks have a strong potential interest for various designs of plasma sources.

(Some figures may appear in colour only in the online journal)

1. Introduction

Plasma processes are widely used in domains such as semiconductors, packaging, solar cells and flat panel displays [1–3]. There is a constant need to improve plasma source performance, especially with regard to larger processed areas and higher process rates. The process rate increase relies essentially on the ability of the plasma sources to generate high electron densities and high dissociation rates of the precursors.

In one approach, parallel plate capacitively coupled reactors were successfully developed for large-area processes. Nowadays, they can deposit thin films on areas of about 2–3 m^2 with a uniformity of ±5% [4]. A major drawback is the low plasma density of capacitively coupled discharges (typically 10^{15}–10^{16} electrons m^{-3}) [5]. Deposition rates are limited because the high ion bombardment energy associated with high voltage sheaths can damage the growing film.

In another approach, the development of inductively coupled plasma (ICP) sources was motivated by the requirement of high densities (in the order of 10^{18} m^{-3}) and dissociation rates [6]. The first inductive plasmas for relatively large-area processes were generated by spiral inductive couplers. Electrical problems arise, however, for diameters above 20–30 cm due to the high RF voltages required at the feeding of the inductor to sustain the high plasma density. The 'ladder antenna' was developed as an alternative

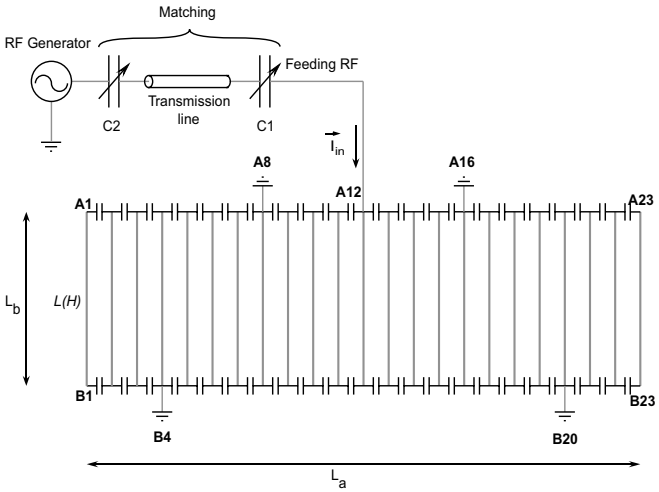

Figure 1. Electrical schema of the planar RF antenna, showing the node numbers and the RF and ground connections. The parallel legs act as inductive elements.

configuration to increase the processed area; its structure of parallel inductive legs can reduce the reactive impedance. The generated plasmas show maximum electron densities of the order of 10^{16} m^{-3} at a power of about 350 W [7].

In this paper, we present a planar, resonant network RF plasma source operating at 13.56 MHz, suitable for both large-area processing and high electron density. It can be designed in principle up to large sizes by adding in series inductive copper legs linked together by capacitors, in contrast to sources [8] where the capacitance is coupled towards the plasma and not in series with the bar inductances. The resulting structure consists of a resonant circuit with modes of excitation characterized by high Q-factors. When the antenna is excited at such a mode frequency, it gives rise to a well-defined distribution of intense RF currents in its parallel legs. A semi-industrial plasma source has been built and tested up to 2 kW. The results demonstrate that it produces a dense and uniform argon plasma by inductive coupling with the resonating currents.

2. Principles of the planar resonant RF network antenna

This section briefly describes the principles of the resonant planar antenna [9]. Its structure is similar to the cylindrical antenna previously described [10, 11], but it has been unwrapped to form an open and planar structure as shown in figure 1. The N parallel legs of the antenna are made of copper tubes which can be taken to act essentially as inductive elements of inductance L. High Q capacitors of capacitance C link the legs together and present also a small inductance M formed by the metallic leads.

Considering the ideal non-dissipative case, the impedances are purely reactive. Solving Kirchhoff's equations over the antenna with the open boundary conditions of the planar structure gives $N-1$ resonant modes m that arise from the network of L and C components. Each mode is characterized by a resonance frequency ω_m and by specific current distributions I_n in the legs and voltage distributions V_{A_n} and V_{B_n} at the nodes A_n and B_n, respectively. For the antenna equivalent circuit represented in figure 1, the resonance frequencies are given by [10]

$$\omega_m = \frac{1}{\sqrt{C\left(M + 2L\sin^2\left(\frac{m\pi}{2N}\right)\right)}}, \qquad \text{with} \quad m \in [1, N-1]. \tag{1}$$

In practice, the resonance frequencies are influenced by mutual inductances between the antenna elements which are not shown in figure 1; they can be accounted for by a matrix approach [10]. When the antenna is excited at one of its resonance frequencies by an excitation potential $V_0\cos(\omega_m t)$ applied to any pair of nodes A_{N_f} and A_{N_g}, the normal mode expressions for the leg currents and node voltages are, respectively, given by

$$\begin{aligned} I_n &= \frac{2V_0}{DL\omega_m}\cdot\cos(k_m(2n-1))\sin(\omega t) \\ V_{A_n} &= -V_{B_n} = \frac{V_0}{D}(\cos(k_m(2n-1)) \\ &\quad -\cos(k_m(2N_g-1)))\cos(\omega t) \end{aligned} \tag{2}$$

where $k_m = m\pi/2N$ and $D = \cos(k_m(2N_f-1)) - \cos(k_m(2N_g-1))$.

The currents and voltages all oscillate sinusoidally in phase, with wavelength inversely proportional to the mode number m. In contrast to the resonance frequency values, the distribution of currents and voltages in equation (2) are almost unaffected by the mutual inductances [10]. The general concept of a resonant RF network opens up a rich field of investigation into diverse types of plasma sources. This paper presents one specific example as a proof of principle for large-area plasma processing. Further possibilities can be envisaged such as multi-modal operation, multiple excitation frequencies, travelling current wave distributions, for example.

3. Experimental arrangement of a planar resonant RF network antenna

An experimental antenna has been built and tested with argon as working gas up to 2 kW for potential applications in plasma processing. As depicted in figure 1, the antenna consists of 23 copper tubes, length $L_b = 0.2$ m, assembled in parallel over a total length $L_a = 0.55$ m.

The antenna is designed to operate at a fixed RF frequency of 13.56 MHz which is allocated for industrial applications. The influence of mode number on uniformity and density remains to be determined; in this work, mode $m = 6$ was used for a detailed study of the antenna performance because it generates higher RF currents in the legs compared to lower modes for the same RF power, and the measured plasma uniformity was adequate. In order to match the frequency of this particular resonant mode with 13.56 MHz, high RF power capacitor assemblies with equivalent capacitance values of $C = 2600$ pF were soldered to the copper legs by silver leads whose inductance is measured to be $M = 6$ nH. The inductance of each copper leg is 0.156 μH. The antenna is fed by the RF power supply through the central leg A_{12} and is connected to ground at points B_4, A_8, A_{16} and B_{20} (see figure 1).

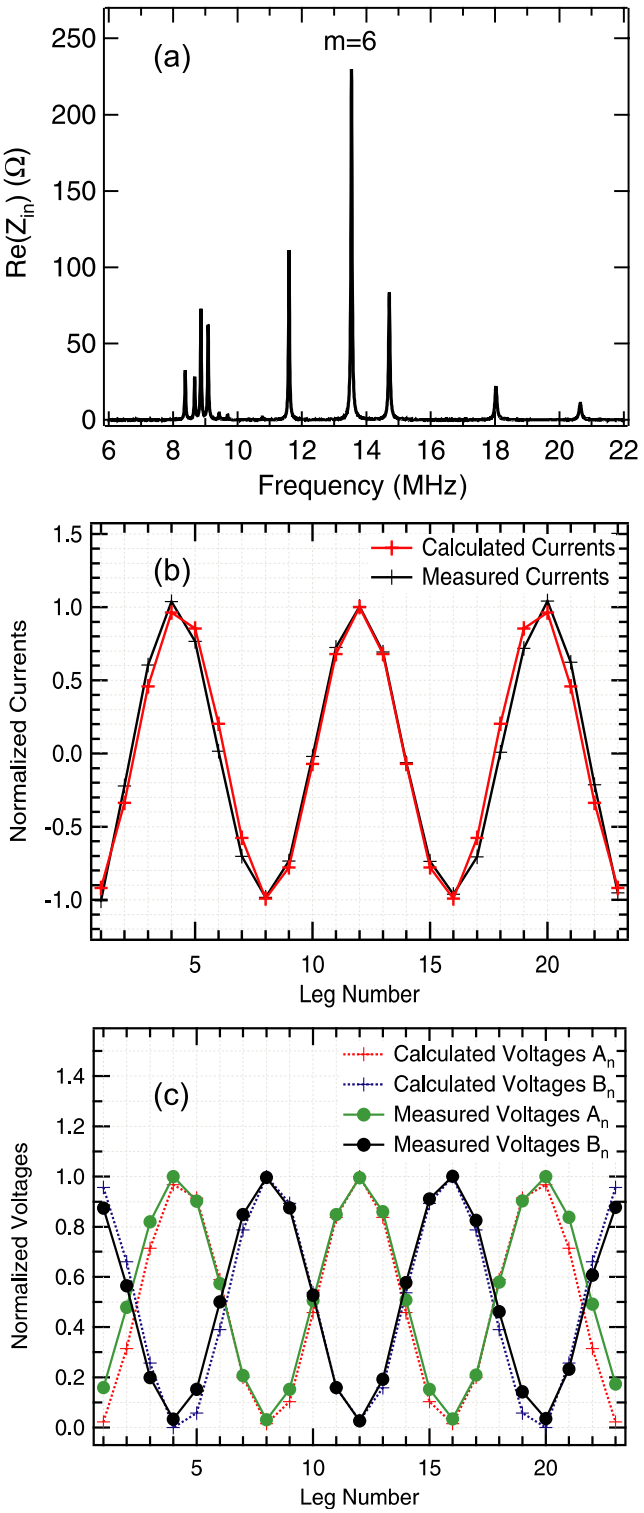

Figure 2. (*a*) Measured resonance spectrum of the 23-leg planar RF antenna without plasma; (*b*) calculated (red) and measured (black) current amplitudes in the legs of the planar RF antenna for the mode $m = 6$. (*c*) Calculated (red and blue dashed lines) and measured (green and black lines) voltage amplitudes at the nodes A_n and B_n for the mode $m = 6$.

The resonance spectrum of the antenna without plasma measured by a network analyser is shown in figure 2(*a*). The resonance frequencies calculated using equation (1) are only approximate (for example, the $m = 6$ mode calculated frequency is 13.25 MHz instead of the measured 13.56 MHz), because of the effect of mutual inductances, and are not shown. Each resonance is characterized by a peak of real impedance and vanishing imaginary impedance. The real impedance for each mode depends on the connection configuration. A feeding configuration at the pair of nodes $A_{N_f=12}$ and $A_{N_g=8}$ was chosen because it maximizes the real part of the antenna impedance for $m = 6$. A high real input impedance value of the antenna implies that the RF input current I_{in} (see figure 1) that flows from the RF generator into the antenna is minimal. This condition is crucial in order to keep the perturbations to the intrinsic resonant currents and voltages distributions (equation (2)) as small as possible. The other three equivalent ground points B_4, A_{16} and B_{20} were connected to ensure symmetric distribution of the input current and to enhance stability of the $m = 6$ mode.

In the presence of plasma, the Q-factor of the resonance modes decreases due to dissipation, and the real impedance value is divided by an estimated factor 5 under strong plasma coupling. The input impedance of the plasma-coupled RF antenna is therefore real and typically in the range 20 to 100 Ω for this frequency and connection configuration, which is convenient for RF matching to a generator with 50 Ω output impedance. In this experiment, the RF power generator is connected to a matching network which consists of a 1 m long coaxial cable in series between two adjustable vacuum capacitors (C1 and C2 in figure 1). The imaginary part of the input antenna impedance Z_{in} is brought to zero by tuning capacitor C2 alone and the real part is brought to 50 Ω by capacitor C1 and the transmission line.

The antenna dimensions can be adapted to larger area processes since the normal mode properties of sinusoidal in-phase currents and voltages with the distributions given by equation (2) do not depend on size. Furthermore, the antenna input impedance is real at a mode frequency, independent of size, and its value can be chosen by design parameters such as the connection configuration. This real input impedance is a key advantage compared with conventional large-area plasma sources because it avoids the problem of strong reactive currents and voltages in the matching box and RF power connections. The antenna legs can be up to metres long before standing wave non-uniformity becomes significant whereupon modifications to the antenna configuration can be made to compensate for this.

In order to characterize the antenna experimentally, the distribution of currents in the legs (using a B-dot probe) and the voltage distributions at the nodes A_n and B_n were measured. It can be seen in figures 2(*b*) and (*c*) that the correspondence between the measurements and the calculated distributions (equation (2)) for the antenna excited in the mode $m = 6$ is excellent. Small discrepancies are observed in the first and last third parts of the antenna; these slight differences are attributed to the mutual inductances between the legs that are not taken into account in the calculations. As expected from the expressions in equation (2) the current distribution is characterized by three wavelengths over the antenna length, symmetric about the central leg.

A linear array of 15 equally spaced single Langmuir probes arranged parallel to the antenna legs was built to

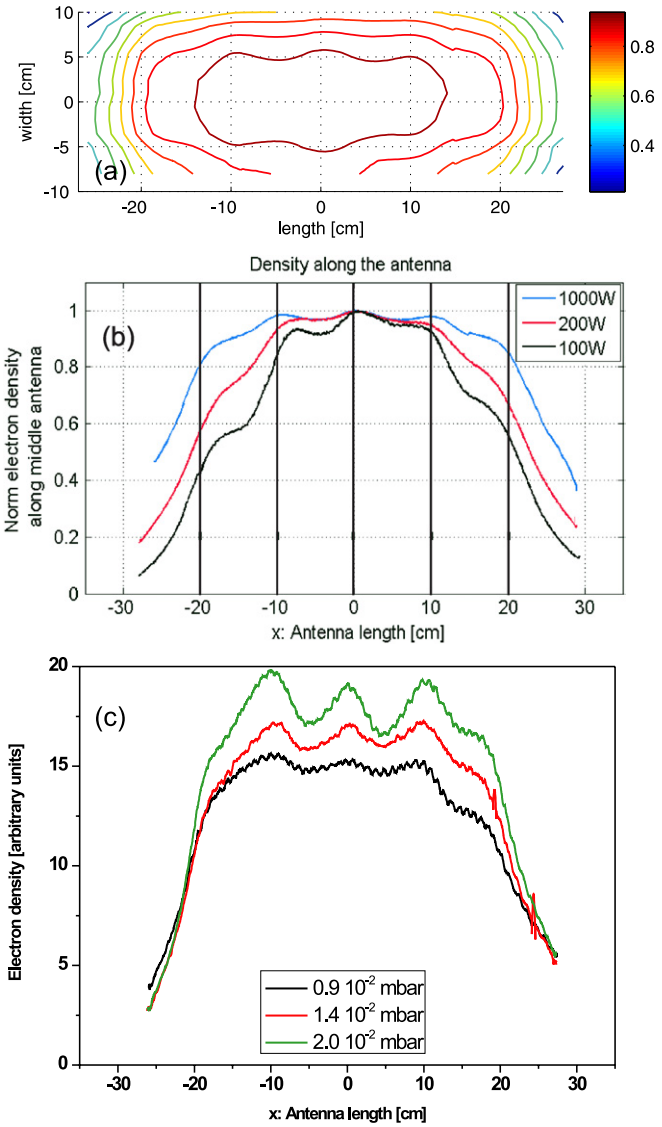

Figure 3. (*a*) Normalized ion density contour profile obtained with Langmuir probes at 4 cm above the antenna for 1000 W RF input power. The contour lines show intervals of 10%. (*b*) Ion density profiles (normalized) along the RF antenna length for 100, 200 and 1000 W. The argon pressure is 0.7×10^{-2} mbar and the flux is 10 sccm. The vertical lines indicate the positions of the legs with maximal currents, nos. 4, 8, 12, 16 and 20, as in figure 2(*b*). (*c*) Ion density profiles at pressures of 0.9×10^{-2}, 1.4×10^{-2}, 2.0×10^{-2} mbar at 175 W in argon.

measure the plasma density profile. The pins are made of steel wires 0.4 mm diameter and 4 mm long. Moving the biased probes through the plasma along the antenna length gives the topography of the ion saturation current which is proportional to the ion and electron density of the argon plasma.

4. Results

For an antenna operating in the mode $m = 6$ at 13.56 MHz, argon plasmas were ignited and sustained with RF power as low as 10 W at pressures between 10^{-3} and 10^{-1} mbar.

Figure 3(*a*) shows the contour lines of ion density measured for an argon plasma at 1000 W along a plane in the middle of the 8 cm gap between the antenna and an electrically floating metal substrate. The uniformity is ±10% over more than 75% of the antenna area.

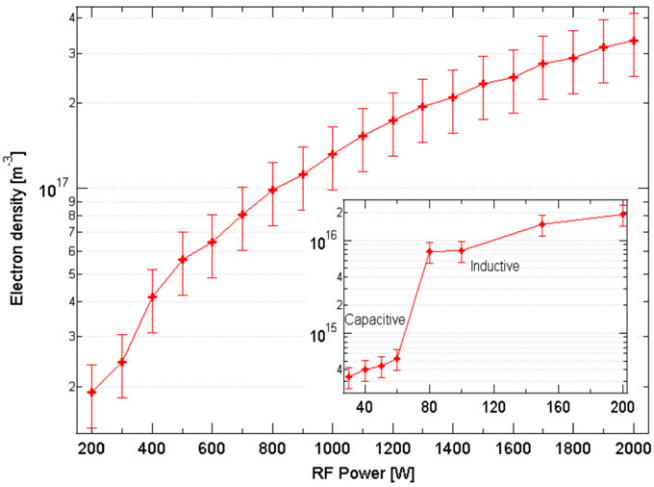

Figure 4. Maximum electron density measured by a 33 GHz interferometer in the argon plasma for RF power increasing from 30 W to 2000 W. The pressure is 10^{-2} mbar and the flux is 30 sccm. The inset shows the transition from capacitive to inductive coupling occurring at around 60 W.

The ion density along the antenna axis is shown in figure 3(*b*). The maxima of the spatial periodic variations of the plasma density, as indicated by the vertical lines, correspond closely to the maxima in the current distribution of the antenna legs in figure 2(*b*), especially at high power. Although the antenna is inductively coupled to the plasma, the image of the antenna current distribution is not very marked in the plasma density at 1000 W in figures 3(*a*) and (*b*). This is related to the low working gas pressure which favors diffusion of the plasma species in the plasma volume. The source image is more strongly visible at higher pressures in figure 3(*c*) where the electron diffusivity is lower; this would also be expected in electronegative gas plasmas due to electron attachment.

Overall, the profiles in figure 3(*b*) broaden with increasing power from 100 to 1000 W. The plasma becomes more uniform with increasing power, possibly because the skin effect begins to limit the inductive coupling efficiency in the centre at high power, whereas the inductive power deposition continues to rise with plasma density [12] near the edges.

The transition from the capacitive mode into the inductive mode was characterized by slowly increasing the RF power and measuring the average electron density along the antenna width using a 33 GHz microwave interferometer. Figure 4 shows the electron density rising above 3×10^{17} m^{-3} at 2000 W, while the inset in Figure 4 shows this evolution between 20 and 200 W. A clear step by more than one order of magnitude in electron density is observed around 60 W for an argon pressure of 10^{-2} mbar. Increasing the argon pressure reduces the power at which this transition occurs. In the inductive mode, the electron density increases monotonically with power and, since no saturation was observed, even higher electron densities should be obtained above 2 kW.

5. Conclusions

A prototype of a resonant planar RF antenna operating at 13.56 MHz has been built and tested up to an RF power of 2000 W. The antenna itself constitutes a resonant structure for which the RF voltages and currents have been completely defined theoretically and measured experimentally with excellent agreement.

Argon plasmas are easily ignited and couple capacitively with the antenna at low power (from 10 to 60 W) and inductively above a threshold power of about 60 W. The maxima of the plasma density profiles correspond closely to the maxima in the antenna current distribution for the mode chosen for excitation, which in this case was the mode $m = 6$. The plasma density uniformity is $\pm 10\%$ over more than 75% of the antenna area above 1000 W. Electron densities above 3×10^{17} m^{-3} were measured by microwave interferometry for an RF power of 2 kW. The real input impedance at antenna resonance avoids the problem of strong reactive currents and voltages in the matching box and RF power connections associated with conventional large-area plasma sources. These promising results encourage further development to increase the area of the antenna as well as the excitation power in order to improve the performance of this type of RF plasma source for industrial applications. The general concept of resonant networks as plasma sources opens up a wide field for investigation.

Acknowledgments

This work was supported by Swiss Commission for Technology and Innovation grant no 9896.2 PFIW-IW.

References

[1] Lieberman M A and Lichtenberg A J 2005 *Principles of Plasma Discharges and Materials Processing* (New York: Wiley-Interscience)
[2] Chatham H 1996 *Surf. Coat. Technol.* **78** 1
[3] Chen F F 2003 *Lecture Notes on Principles of Plasma Processing* (Dordrecht/New York: Kluwer/Plenum)
[4] Schmidt H, Sansonnens L, Howling A A, Hollenstein C, Elyaakoubi M and Schmitt J 2004 *J. Appl. Phys.* **95** 4559
[5] Chabert P and Braithwaite N St. J 2011 *Physics of Radio-Frequency Plasmas* (Cambridge: Cambridge University Press)
[6] Hopwood J 1992 *Plasma Sources Sci. Technol.* **1** 109
[7] Wendt A E and Mahoney L J 1996 *Pure Appl. Chem.* **68** 1055
[8] Lim J H, Kim K N, Park J K and Yeom G Y 2008 *Phys. Plasmas* **15** 083501
[9] Guittienne P 2010 Apparatus for large area plasma processing (August 2010) http://www.sumobrain.com/patents/WO2010092433.html
[10] Jin J 1998 *Electromagnetic Analysis and Designs in Magnetic Resonance Imaging* (Boca Raton, FL: CRC press)
[11] Guittienne P and Chevalier E 2005 *J. Appl. Phys.* **98** 083304
[12] Cunge G, Crowley B, Vender D and Turner M M 1999 *Plasma Sources Sci. Technol.* **8** 576